Adsorption and Entrapment of Salicylamide Molecules into the Mesoporous Structure of Folded Sheets Mesoporous Material (FSM-16)

Yuichi Tozuka,[1,3] Toshio Oguchi,[2] and Keiji Yamamoto[1]

Received December 19, 2003; accepted March 3, 2003

Purpose. The aim of this study was to estimate the molecular state of salicylamide on the surface of mesoporous silicas and to investigate the dissolution behavior of salicylamide from the solid dispersion.
Methods. Folded sheets mesoporous material (FSM-16) were used as a porous material. The molecular state of salicylamide was estimated by powder X-ray diffractometry, infrared spectroscopy, and fluorescence spectroscopy.
Results. The molecular state of salicylamide can be changed by simple blending with FSM-16. When a physical mixture of 25% salicylamide and 75% FSM-16 was heated at 120°C for 3 h, amorphization of salicylamide was observed from the powder X-ray diffraction pattern. The fluorescence emission peak of salicylamide at 433.5 nm shifted to a longer wavelength of 447.5 nm after heating. Changes in fluorescence decay curve suggested that salicylamide molecules were dispersed into the hexagonal FSM-16 channels during the heating process. Enhanced dissolution in the initial stage of salicylamide from the sealed heated sample was observed in comparison with salicylamide crystals.
Conclusions. Heat treatment of a physical mixture of salicylamide with FSM-16 gave a solid dispersion in which the salicylamide molecules changed to an amorphous state by adsorption onto the FSM-16 channels. Amorphization of salicylamide contributed to the improvement of dissolution.

KEY WORDS: porous material; fluorescence spectrum; fluorescence lifetime; salicylamide; FSM-16.

INTRODUCTION

Many medicines developed in recent years are poorly water-soluble compounds. The enhancement of oral bioavailability of poorly water-soluble compounds remains one of the most challenging aspects of drug development. To improve the dissolution profile of poorly water-soluble compounds, we have investigated the use of porous materials as pharmaceutical excipients (1,2). Porous materials have unique properties of adsorptive ability for a variety of organic compounds due to their huge specific surface area and porous texture. Activated carbon is widely known as a representative porous material and has been applied for pharmaceutical use (3). When organic compounds were adsorbed onto the surface of porous material, the organic compounds changed their physicochemical properties, such as stability and dissolution properties (1,4). To control the stability or the dissolution behavior of a medicine, regulation of the molecular state of the medicine is indispensable in solid dispersion. For this reason, it is necessary to understand the molecular state of medicines in solid dispersion systems.

Folded sheets mesoporous material (FSM-16), mesoporous silica having a uniform porous structure of well-defined distribution, has newly been synthesized by using micelle (5,6). FSM-16 is composed of ''honeycomb-like'' hexagonal channels and indicates extremely large specific surface area. In industrial chemistry, the use of FSM-16 as a catalyst has been reported (7,8). However, there was few or no report with regard to its application for pharmaceutical use. When porous materials are handled, the porous structure could be changed or broken during grinding or tableting. However, with regard to FSM-16, Ishikawa *et al.* reported that the mesoporous structure was maintained after being pressed at pressures below 780 kg cm^{-2} (9). Therefore, the focus of this study is on the application of FSM-16 for pharmaceutical use.

Salicylamide, a medicine for analgesic use, was used as a model compound. In our present study, molecular state changes of salicylamide molecules in the presence of FSM-16 was estimated by using X-ray diffractometry, IR spectroscopy, and fluorescence spectroscopy. The pharmaceutical application of FSM-16 was evaluated by the dissolution study.

MATERIALS AND METHODS

Materials

Salicylamide (Nacalai Tesque, Kyoto, Japan) of reagent grade was used without further purification. Mesoporous silica FSM-16 (mean pore width of 2.1 nm, specific surface area of 1,250 m^2/g) was kindly supplied by Toyota Central R&D Labs., Inc., Japan. FSM-16 was sieved using a 200-μm aperture size sieve and was used after drying under a reduced pressure at 110°C for 3 h. Physical mixtures were prepared by blending of salicylamide and FSM-16 in a glass vial for 1 min. A physical mixture (about 250 mg) was sealed in a glass ampoule (2 mL) and then heated at 120°C for 3 h to prepare a sealed-heated sample.

Powder X-Ray Diffractometry

Powder X-ray diffraction was performed using a Rigaku Miniflex diffractometer (Tokyo, Japan). The measurement conditions were as follows: target, Cu; filter, Ni; voltage, 30 kV; current, 15 mA; scanning speed, 2°/min.

Fourier-Transformed Infrared (FT-IR) Spectroscopy

FT-IR spectra were measured by the KBr disc method at a resolution of 2 cm^{-1} for 32 scans using a JASCO 230 FT-IR spectrophotometer (Tokyo, Japan).

Fluorescence Spectroscopy

An FP-770F fluorescent spectrometer (Japan Spectroscopy Co., Ltd., Tokyo, Japan) was used for stationary fluorescence spectroscopy. Powder samples were filled into a front-face reflectance cell (FP-1060).

[1] Graduate School of Pharmaceutical Sciences, Chiba University, 1-33 Yayoicho, Inage-ku, Chiba 263-8522, Japan.
[2] Department of Pharmacy, Yamanashi University, 1110 Tamahocho, Nakakoma-gun, Yamanashi 409-3898, Japan.
[3] To whom correspondence should be addressed. (e-mail: ytozuka@p.chiba-u.ac.jp)

0724-8741/03/0600-0926/0

Determination of the Fluorescence Lifetime and Relative Quantum Yield

Fluorescence decay profiles were measured by a nanosecond time-resolved single-photon counter with a pulse width of 1.5 ns (Horiba NAES-770, Tokyo, Japan). The exciting pulse and emission response functions were measured simultaneously, and the decay parameters were calculated from two or three exponential functions obtained by deconvolution of the excitation pulse profile using a non-linear least-squares fitting. The goodness of fit was assessed by monitoring value of χ^2 and the distribution of residuals.

Differential Scanning Calorimetry

A differential scanning calorimeter (DSC, Model DSC3100S, MAC Science, Japan) was used. The operating conditions in the closed- aluminum pan system were as follows: sample weight, 3 mg; heating rate, 5°C/min; without nitrogen gas flow.

Dissolution Study

Dissolution studies were performed according to the Japanese Pharmacopoeia (JP) XIV paddle method. Distilled water of 500 mL was used as a dissolution medium thermostated at 37.0°C. The paddle revolution speed was adjusted to 50 rpm. At definite intervals, 3 ml of the solution was pipetted out and filtered through a membrane filter of 0.45 μm. The concentration of salicylamide was determined spectrophotometrically at 302.8 nm by using a UV-visible recording spectrometer (UV-160, Shimadzu, Japan).

Results and Discussion

The powder X-ray diffraction patterns of salicylamide, FSM-16, and mixtures of salicylamide and FSM-16 (salicylamide content = 25%) are shown in Fig. 1. The diffractogram of the physical mixture of 25% salicylamide and 75% FSM-16 was a superimposed pattern of salicylamide crystals and FSM-16. By heating the physical mixture, the intensity of the diffraction peaks of salicylamide gradually decreased with an increase in heating time. When the physical mixture of 25% salicylamide and 75% FSM-16 was heated at 120°C for 3 h (as shown in Fig. 1d), powder X-ray diffraction peaks resulting from crystalline salicylamide completely disappeared, whereas the powder X-ray diffraction peaks resulting from crystalline salicylamide clearly remained for the 50% and 75% salicylamide- FSM-16 systems. These results indicated that salicylamide crystals changed to the amorphous state by heating. For a clear understanding of the adsorption mode of salicylamide, it is important to know the interaction mode between salicylamide and FSM-16. Figure 2 shows the IR spectra of salicylamide with FSM-16 systems (salicylamide content = 25, 50, 75%). The absorption band observed at 1675 cm^{-1} at the spectrum of salicylamide crystals was assigned to the carbonyl stretching vibration (10,11). The transmittance of this peak (indicated by a closed star) weakened gradually as the salicylamide content decreased. The physical mixture of 25% salicylamide and 75% FSM showed a new peak at 1658 cm^{-1} (indicated by an arrow) with a shoulder peak of carbonyl stretching vibration of salicylamide crystals. This indicated that two kinds of molecular interaction mode would exist even in the physical mixture. Simple blending might cause a drastic change in the molecular state of salicylamide. After sealed-heating the physical mixture of 25% salicylamide and 75% FSM, only the new absorption peak at 1658 cm^{-1} was observed in the IR spectrum, while the peak at 1675 cm^{-1} disappeared. Salicylamide crystals have been reported to show intermolecular hydrogen bond with the characteristic peak at 1687 cm^{-1} (11). The hydrogen bond network in the salicylamide crystal would break after the heating followed by a new hydrogen bond between the silanol groups of FSM-16 and the salicylamide molecules adsorbed.

Figure 3 shows the fluorescence emission spectra of salicylamide with FSM-16 systems when the excitation wavelength was fixed at 262.7 nm. The fluorescence emission peak of salicylamide crystals was observed at 433.5 nm. When the salicylamide crystals were sealed-heated with FSM-16 for 3 h, the emission peak at 433.5 nm gradually shifted to longer

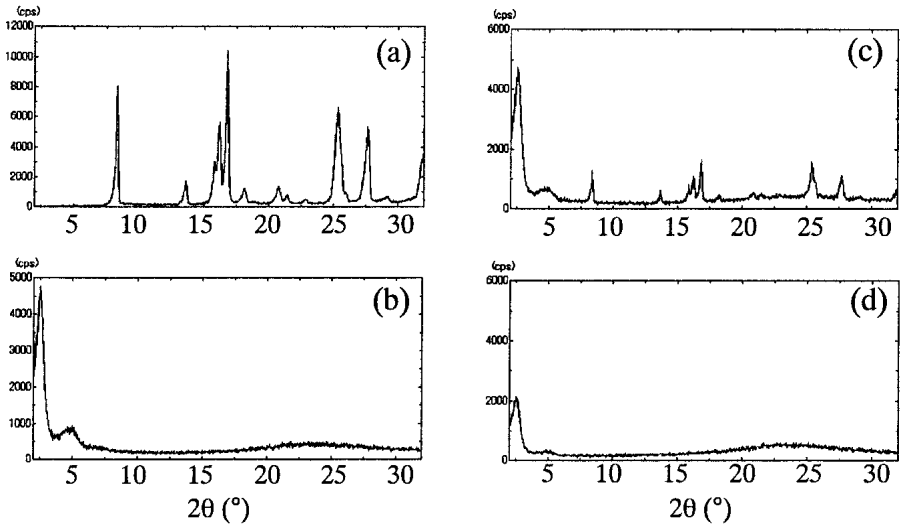

Fig. 1. Change in the powder X-ray diffraction patterns of salicylamide–FSM-16 systems. (a) Salicylamide crystals; (b) FSM-16; (c) physical mixture of 25% salicylamide-75%FSM-16; (d) sealed heated sample of 25% salicylamide--75% FSM-16.

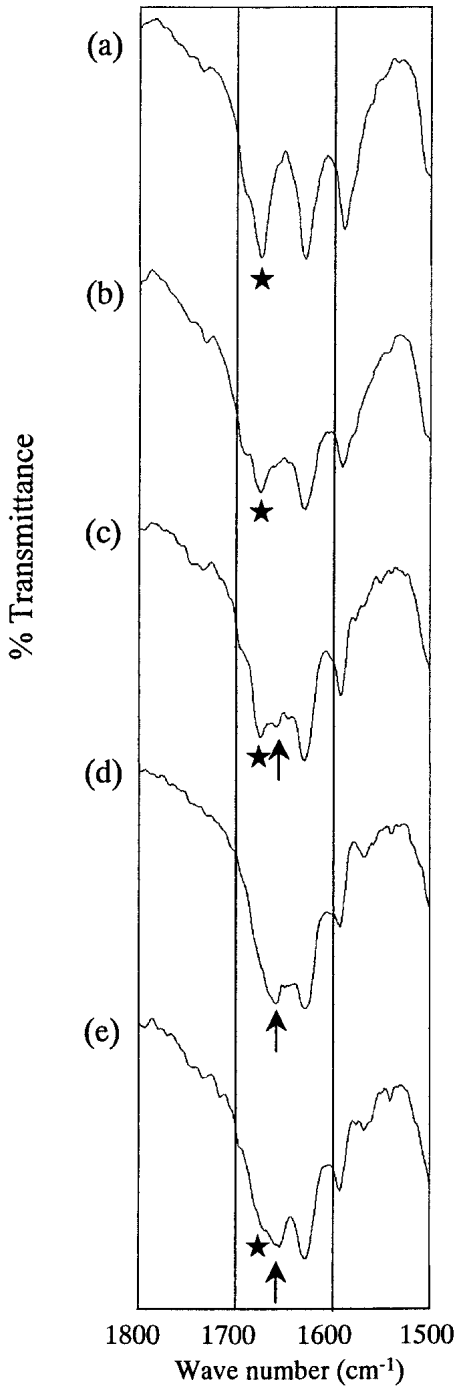

Fig. 2. Changes in the infrared spectra of salicylamide–FSM-16 systems. (a) Salicylamide crystals; (b) scaled-heated sample of 75% salicylamide–25% FSM-16; (c) sealed-heated sample of 50% salicylamide–50% FSM-16; (d) sealed-heated sample of 25% salicylamide–75% FSM-16; (e) physical mixture of 25% salicylamide–75% FSM-16.

wavelengths with the decrease in salicylamide content. In the 25% salicylamide–75% FSM-16 system, the emission peaks of the physical mixture and of the sealed-heated sample were observed at 441.5 and 447.5 nm, respectively. Because the emission peak of the physical mixture was shifted to a longer wavelength in comparison with salicylamide crystals, it seemed likely that simple blending with FSM-16 caused the

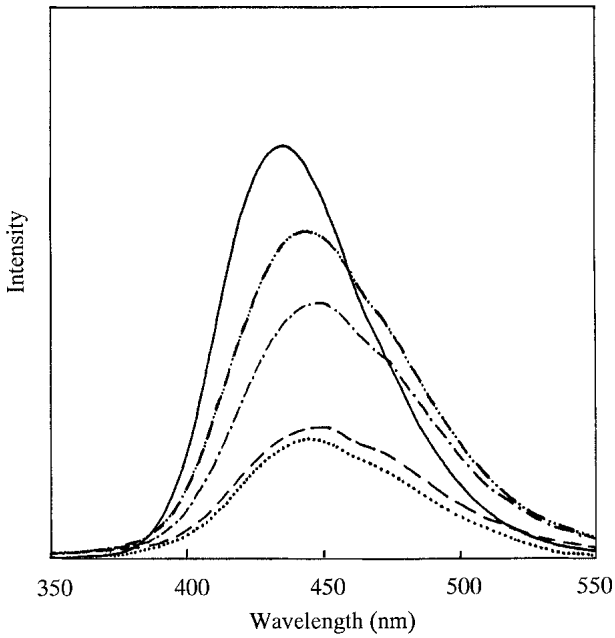

Fig. 3. Solid-state fluorescence emission spectra of salicylamide–FSM-16 systems after the sealed-heating at 12°C for 3 h; λex = 262.7 nm. Salicylamide crystals (solid line); 75% salicylamide–25% FSM-16 (-···-); 50% salicylamide–50% FSM-16 (-··-); 25% salicylamide–75% FSM-16 (-·-·); physical mixture of 25% salicylamide–75% FSM-16 (····).

molecular state change of salicylamide. In our previous article (12), we reported that 2-naphthoic acid showed the emission peak shift to longer wavelength when the 2-naphthoic acid molecules were adsorbed monomolecularly onto porous crystalline cellulose. The emission peak observed at a longer wavelength than that of the crystals would be caused by salicylamide molecules adsorbed onto the FSM-16. The IR and fluorescence emission spectra represented the remarkable spectral changes in the physical mixture, although the X-ray diffraction pattern of the physical mixture showed the diffraction peaks of salicylamide crystal as shown in Fig. 2. These results indicated that salicylamide molecules partly adsorbed on the surface of FSM and partly remained as the crystals after the mixing with FSM-16 for 1 min. By means of molecular simulation studies based upon the grand canonical Monte Carlo simulation method, Kaneko *et al.* showed that micropores generally have stronger adsorption field (13–16). In micropores, an enhanced adsorption of vapor molecules such as methanol and methane was observed even in a low relative pressure range. Since the pore diameter of FSM-16 used was approximately classified as micropores (2.1 nm), it was presumed that the rapid adsorption of salicylamide was responsible for the peculiar adsorptive ability of FSM-16, though the vapor pressure of salicylamide was considered to be comparatively low.

To investigate the molecular state change of salicylamide in detail, fluorescence decay kinetics was performed. We attempted to compare the lifetime data to advance our discussion concerning the adsorption mode of salicylamide. Figure 4 exhibits the changes in fluorescence decay curves of salicylamide in the systems with FSM-16. In the 25% salicylamide–75% FSM system, the fluorescence decay curve from salicylamide in the sealed-heated sample was different from that of

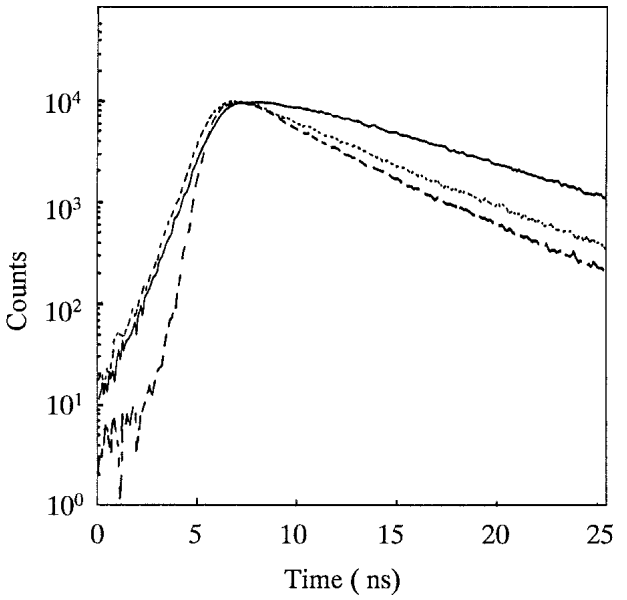

Fig. 4. Fluorescence decay curves, λex = 262.7. Salicylamide crystals (solid lines); physical mixture of 25% salicylamide–75% FSM-16 (····); sealed-heated sample of 25% salicylamide-75% FSM-16 (---).

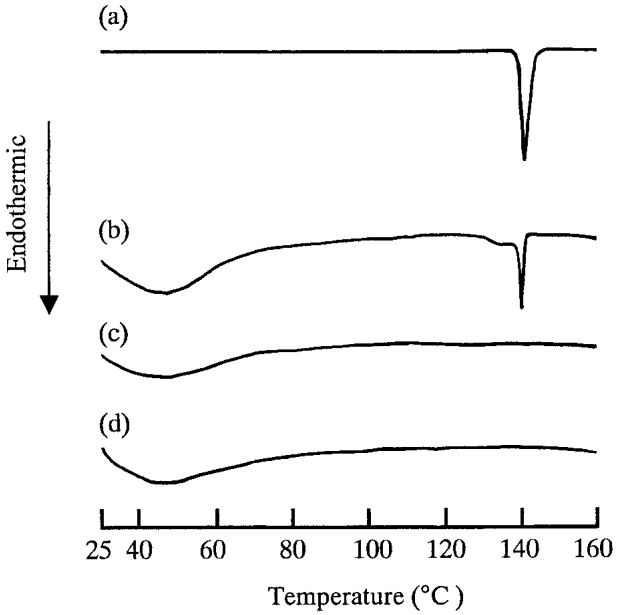

Fig. 5. Differential scanning calorimetry of 25% salicylamide–75% FSM-16 system. (a) Salicylamide crystals; (b) physical mixture (first run); (c) physical mixture (second run); (d) heated sample.

the physical mixture. Furthermore, the slopes of fluorescence decay curves increased in the order of salicylamide crystals, the physical mixture, and sealed-heated sample. The fluorescence decay curve of sealed-heated sample was well-fitted by use of two exponential functions, whereas the fluorescence decay curve of physical mixture did not give a good fitting parameter if the deconvolution was performed using two exponential functions. By calculating from three exponential functions, the physical mixture gave a good value for the fitting parameter (χ^2 <1.3). The fluorescence lifetime and relative quantum yield of salicylamide in the salicylamide–FSM-16 system are listed in Table I. The component of short lifetime (τ_1 <0.3 ns) of the salicylamide crystals could be due to stray light (17). The long lifetime component of salicylamide (τ_2: 6~7 ns) represented the dominant component of the salicylamide crystals. This result was indicative of the existence of two kinds of molecular species of salicylamide in the physical mixture. Compared with the changes in fluorescence spectra and IR spectra (Figs. 2 and 3), the short-lifetime component (τ_3: 2~3 ns) was caused by the salicylamide molecules adsorbed in the hexagonal structure of FSM-16.

Figure 5 illustrates the DSC thermograms of salicylamide of the 25% salicylamide–75% FSM-16 system at a heating rate of 5°C/min. Salicylamide crystal exhibited only an endothermic peak due to melting at 140°C. The physical mixture of 25% salicylamide and 75% FSM-16 showed a different thermal behavior from the salicylamide crystals. The broad peak around 25–60°C was attributed to dehydration from FSM-16, two endothermic overlapping peaks were observed around 140°C: the first was broad and observed at a lower temperature compared to the melting point of salicylamide crystals and the second was due to the melting of salicylamide crystals. However, the second run of the physical mixture and the sealed-heated sample showed no melting endothermic peak of salicylamide crystals. Yonemochi *et al.* reported that three different states of benzoic acid would exist in a mixture of benzoic acid and controlled-pore glass having a pore diameter of 12 nm (18). The three states were crystalline state (phase 1), the disordered crystalline state for which a broad endothermic peak was observed at a lower temperature (phase 2), and the amorphous state for which no peak on the DSC curves was observed (phase 3). The DSC thermogram of the physical mixture of 25% salicylamide and 75% FSM-16 indicated the existence of phase 1 and phase 2 of salicylamide. For the sample cooled from high temperature (>140°C) to room temperature, e.g., the second run of the physical mixture or the sealed-heated sample, the salicylamide molecules existed in phase 3 and exhibited no melting peak in the DSC curve. These results supported that the salicylamide crystals changed to the amorphous state during the heating procedure.

Dissolution properties of salicylamide in distilled water were studied according to the JP XIV paddle method and the results are shown in Fig. 6. In the initial stage of dissolution, the sealed-heated sample exhibited faster dissolution rate than that of salicylamide crystals. With regard to the sealed-heated sample, salicylamide were physically adsorbed in the pores of FSM-16 and an activated state of salicylamide should

Table I. Fluorescence Lifetime (τ) and Relative Quantum Yield (Q) of 25% Salicylamide–FSM-16 System, λex = 262.7 nm

Sample	λ_{obs} (nm)	τ_1 (ns)	Q_1 (%)	τ_2 (ns)	Q_2 (%)	τ_3 (ns)	Q_3 (%)	χ^2
Salicylamide crystals	433.5	0.292	23.7	6.36	76.3			1.30
Physical mixture	445.5	0.484	38.4	7.48	16.7	2.35	44.9	1.12
Sealed-heated sample	447.0	0.807	52.4			3.37	47.6	1.18

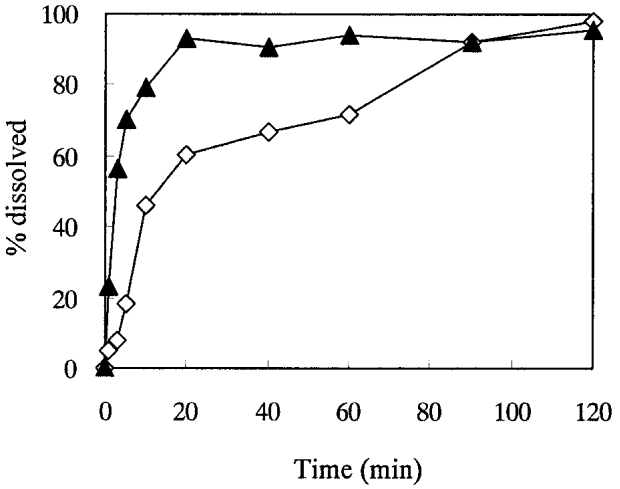

Fig. 6. Dissolution profiles of salicylamide from salicylamide crystals (◇) and sealed-heated samples of 35% salicylamide–75% FSM-16 (▲).

contribute to the improvement of dissolution. Since the surface properties of FSM-16 were sensitive to moisture (19), the wettability of FSM-16 surface was higher than that of salicylamide crystals. Moreover, water molecules affected the dissolution of salicylamide from the sealed heated sample through the ability to adsorb on pores of FSM-16 and to destroy the molecular interaction between FSM-16 and salicylamide.

CONCLUSIONS

The physicochemical properties of salicylamide were changed by simple blending and by heating with FSM-16. The adsorptive ability of FSM-16 micropores might promote the rapid adsorption of salicylamide. From the thermal analysis, it was found that the salicylamide adsorbed could exist in an amorphous state stably. It was revealed that the solid dispersion of salicylamide and FSM-16 was useful in achieving fast dissolution of salicylamide.

ACKNOWLEDGMENTS

The authors would like to thank Toyota Central R&D Labs., Inc., Japan for the kind gift of FSM-16. This work was supported in part by a Grant-in-Aid for Scientific Research from the Ministry of Education, Culture, Sports, Science and Technology, Japan (12672085)

REFERENCES

1. S. Okonogi, T. Oguchi, E. Yonemochi, S. Puttipipatkhachon, and K. Yamamoto. Improved dissolution of ofloxacin via solid dispersion. *Int. J. Pharm.* **156**:175–180 (1997).
2. T. Oguchi, Y. Tozuka, S. Okonogi, E. Yonemochi, and K. Yamamoto. Improved dissolution of naproxen from solid dispersions with porous materials. *J. Pharm. Sci. Technol. Jpn.* **57**:168–173 (1997).
3. J. M. Kisler, A. Dähler, G. W. Stevens, and A. J. O'Connor. Separation of biological molecules using mesoporous molecular sieves. *Micropor. Mesopor. Mater* **44-45**:769–774 (2001).
4. K. Matsumoto, Y. Nakai, E. Yonemochi, T. Oguchi, and K. Yamamoto. Aspirin hydrolysis in mixtures with porous crystalline cellulose. *Drug Stability* **1**:93–97 (1996).
5. Y. Fukushima and S. Inagaki. Nano-scale structure control of mesoporous silica. *Mater. Sci. Eng. A* **217-218**:116–118 (1996).
6. Y. Sakamoto, S. Inagaki, T. Ohsuna, N. Ohnishi, Y. Fukushima, Y. Nozue, and O. Terasaki. Structure analysis of mesoporous material 'FSM-16' Studies by electron microscopy and X-ray diffraction. *Micropor. Mesopor. Mater.* **21**:589–596 (1998).
7. D. Shouro, Y. Moria, T. Nakajima, and S. Mishima. Mesoporous silica FSM-16 catalysts modified with various oxides for the vapor-phase beckmann rearrangement of cyclohexanone oxime. *Appl. Catal. A: Gen.* **198**:275–282 (2000).
8. A. Fukuoka, N. Higashimoto, Y. Sakamoto, and S. Inagaki. Y.i Fukushima, and M Ichikawa. Preparation and catalysis of Pt and Rh nanowires and particles in FSM-16. *Micropor. Mesopor. Mater* **48**:171–179 (2001).
9. T. Ishikawa, M. Matsuda, A. Yasukawa, K. Kandori, S. Inagaki, T. Fukushima, and S. Kondo. Surface silanol groups of mesoporous silica FSM-16. *J. Chem. Soc. Faraday Trans.* **92**:1985–1990 (1996).
10. J. Palomar and J. L. G. De Paz. and J. Catalan. Vibrational study of intramolecular hydrogen bonding in *o*-hydroxybenzoil compounds. *Chem. Phys.* **246**:167–208 (1999).
11. Y. Sasada and T. Takano, and M. Kakudo. Crystal structure of Salicylamide. *Bull. Chem. Soc. Jpn.* **37**:940–946 (1964).
12. Y. Tozuka, E. Yonemochi, T. Oguchi, and K. Yamamoto. Molecular states of 2-naphthoic acid in solid disersions with porous crystalline cellulose, as investigated by fluorescence spectroscopy. *Bull. Chem. Soc. Jpn.* **73**:1567–1572 (2000).
13. K. Kaneko. Molecular assembly formation in a solid nanospace. *Colloids Surfaces A: Physicochem. Eng. Aspects* **109**:319–333 (1996).
14. T. Ohkubo, T. Iiyama, and K. Kaneko. Organized structures of methanol in carbon nanospaces at 303 K studies with in situ X-ray diffraction**.** *Chem. Phys. Lett.* **312**:191–195 (1999).
15. T. Suzuki, R. Kobori, and K. Kaneko. Grand canonical Monte Carlo simulation-assisted pore-width determination of molecular sieve carbons by use of ambient temperature N_2 adsorption. *Carbon* **38**:630–633 (2000).
16. J. Miyawaki and K. Kaneko. Pore width dependence of the temperature change of the confined methane density in slit-shaped micropores. *Chem. Phys. Lett.* **337**:243–247 (2001).
17. Y. Tozuka, E. Yonemochi, T. Oguchi, and K. Yamamoto. Fluorescence studies of pyrene adsorption on porous crystalline cellulose. *J. Colloid Interface Sci.* **205**:510–515 (1998).
18. E. Yonemochi. M Kojinma, A. Nakatsuji, S. Okonogi, T. Oguchi, Y. Nakai, and K. Yamamoto. Thermal behavior of methyl p-hydroxybenzoate in controlled-pore glass solid dispersion. *J. Colloid Interface Sci.* **173**:186–191 (1995).
19. A. Matsumoto, T. Sasaki, N. Nishijima, and K. Tsutsumi. Thermal stability and hydrophobicity of mesoporous silica FSM-16. *Colloids and Surfaces A. Physicochem. Eng. Aspects* **203**:185–193 (2002).